

## **Comparison of vinculin tension in cellular monolayers and three-dimensional multicellular aggregates: supplement**

**LUNI HU,<sup>1</sup> RICK I. COHEN,<sup>1</sup> MARGARIDA BARROSO,<sup>2</sup> AND NADA N. BOUSTANY<sup>1,\*</sup>**

<sup>1</sup>*Department of Biomedical Engineering, Rutgers University, Piscataway, NJ 08854, USA*

<sup>2</sup>*Department of Molecular and Cellular Physiology, Albany Medical College, Albany, NY 12208, USA*

\**nboustan@rutgers.edu*

---

This supplement published with Optica Publishing Group on 13 August 2024 by The Authors under the terms of the [Creative Commons Attribution 4.0 License](#) in the format provided by the authors and unedited. Further distribution of this work must maintain attribution to the author(s) and the published article's title, journal citation, and DOI.

Supplement DOI: <https://doi.org/10.6084/m9.figshare.26501347>

Parent Article DOI: <https://doi.org/10.1364/BOE.529156>

## COMPARISON OF VINCULIN TENSION IN CELLULAR MONOLAYERS AND THREE-DIMENSIONAL MULTICELLULAR AGGREGATES: SUPPLEMENTAL DOCUMENT

### 1. Image processing details

Figure S1 depicts the image processing steps leading to the calculation of lifetime in the segmented regions of interest (ROIs).

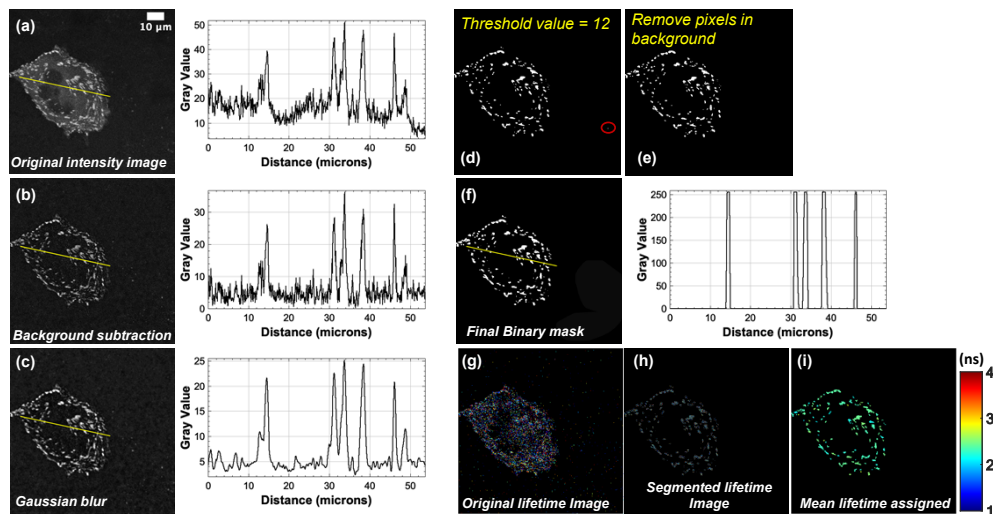


Fig. S1. The processed image and corresponding profile at each step. (a) The original intensity image of a cell expressing VinTS (left panel) and the gray value profile along the yellow line of the image (right panel). (b) Processed image and profile after background subtraction (rolling ball with  $r = 30$  pixels). (c) Processed image and profile after Gaussian Blur (Sigma = 2 pixels). (d) A threshold value (12 in this example) was set in Panel (c) to exclude most of the pixels falling in the background. (e) Any remaining point (red circle) falling outside the cell is manually removed. (f) Processed image and profile after creation of the final binary mask. This step includes manual removal of the spurious signals outside the cell region. (g) Original lifetime image, (h) Processed image after multiplying the binary mask with the original lifetime image. (i) Processed lifetime image after assigning the intensity-weighted mean value within each focal adhesion region to that same region.

To obtain the binary image (going from Panel (c) to Panel (f) in the above example), a manual threshold value was used and varied depending on the intensity of the original image. The threshold was chosen so that most of the pixels falling in the background were eliminated. In the example above, the threshold value was set at 12 in Panel (c). Any remaining spurious signals outside the cell region are manually removed.

### 2. Confocal microscopy channel cross talk

To examine the possibility of experimental errors caused by crosstalk between the fluorescence of the VinTS detected in the Alexa 488 channel and the secondary antibody detected in the Alexa 647 channel, we compared the fluorescence intensity of the VinTS probe under 488nm and 633nm excitation (**Figure S2a**) in a sample labeled with VinTS only and under the same image acquisition conditions as the data in **Fig. 1**. The analysis of five images (**Figure S2b**) revealed that the signal in the Alexa 647 channel is 6.85% of the signal measured in the Alexa 488 channel. However, the pattern of fluorescence appears different in the red and green channels, indicating that the signal detected in the red channel may not be due to cross-talk per

se, but perhaps caused by non-specific autofluorescence when excited at 633nm. As such and given the very low level of cross-talk ( $\sim 7\%$ ), the cross-talk was considered negligible and a cross-talk correction was not implemented.

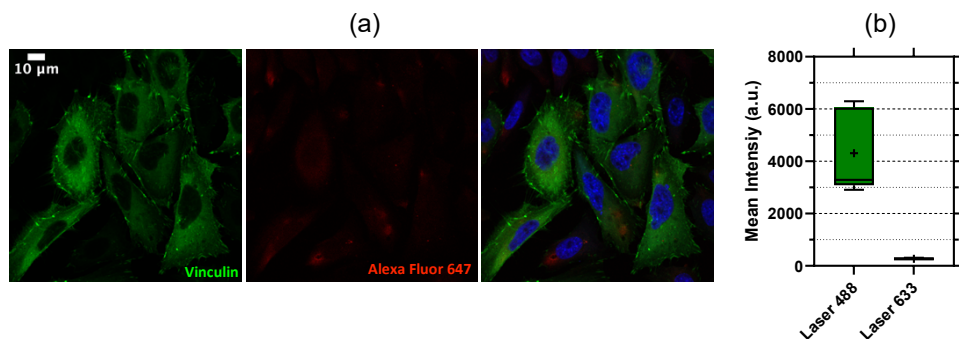


Fig. S2. Quantitative analysis of crosstalk was performed in CHO-K1 monolayers expressing VinTS. (a) Representative images of VinTS were obtained using excitation wavelengths of 488nm (green) and 633nm (red). The vinculin channel was captured with a laser power of 18%-28% and gain of 600-800 in the emission range of 498nm-535nm (in Fig. 1 the 488 nm laser power was 20%). The red channel was acquired with a laser power of 30% and gain of 700 in the emission range of 649nm-700nm. (b) Box and Whiskers plot of intensities measured in the two channels. The whiskers denote minimum and maximum values. The line denotes the median and the box length corresponds to the interquartile range. The crosstalk ratio was calculated by dividing the mean intensity at 633nm by the mean intensity at 488nm.

### 3. Representative volume rendering of multicellular aggregates intensity and lifetime

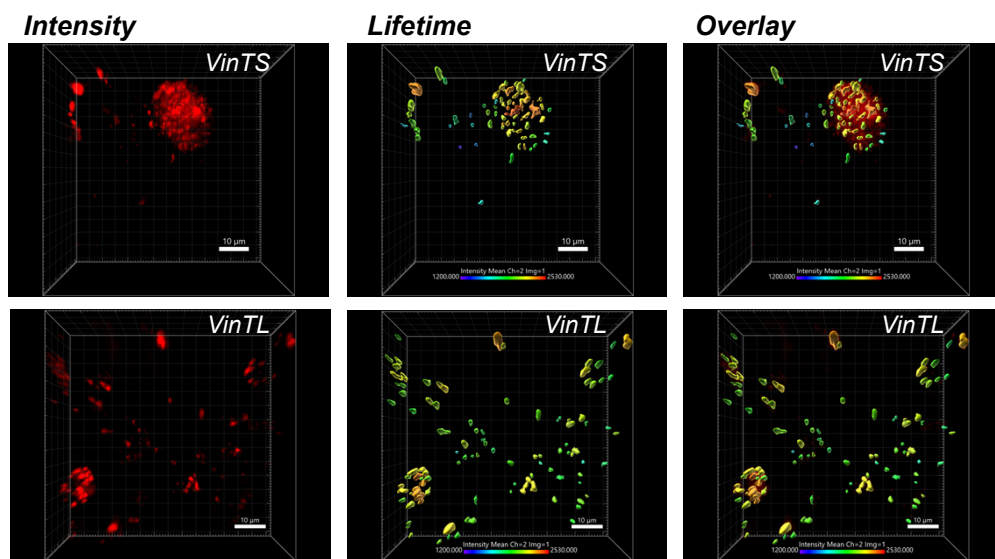


Fig. S3. Volume rendering of representative multicellular aggregates corresponding to the samples shown in Fig. 3. Left Panels: Donor intensity, Middle Panels: Corresponding fluorescence lifetime, Right Panels: Overlay of intensity and lifetime channels. Color scale denotes lifetime in nanoseconds multiplied by 1000. (Images generated with Imaris, Oxford Instruments)

#### 4. Photobleaching:

Our FLIM system is equipped with two channels with lasers exciting the sample at 450nm and 520nm. While we only used the Donor channel (at 450nm excitation) to obtain lifetime and FRET efficiency values in the course of this study, the 520nm laser was left on to check for mVenus fluorescence in the acceptor channel. When the laser at 520nm (mVenus) was turned off, the lifetime of TSMoD significantly decreased (from 2.25ns to 2.16ns) in 2D monolayers but remained unchanged (from 2.11ns to 2.14ns) in the 3D multicellular aggregates. Moreover, after turning off the 520nm laser, the TSMoD measurements in the 2D monolayers showed no significant difference compared to those in the 3D multicellular aggregates (**Fig. S4.a**). Thus, the acceptor fluorophore in the TSMoD construct is sensitive to photobleaching in the 2D monolayers when the 520nm laser is turned on. However, further photobleaching tests on VinTL showed that the lifetime of VinTL was not changed (from 2.175ns to 2.174ns) in 2D monolayers when the 520nm laser was turned off (**Figure S4.b**). We therefore assumed that, unlike TSMoD, VinTL and VinTS are not affected by photobleaching in the 2D cultures. As a result, conversion of lifetime to FRET efficiency was performed using the TSMoD data collected from the 3D aggregates, and which are equivalent to the 2D monolayers TSMoD data acquired with the 520nm turned off (**Fig. S5 and 5d**). Had we used a different conversion for the 2D cultures using the TSMoD data measured in the 2D cultures with the 520nm turned on, the mean FRET efficiency of VinTL and VinTS in the 2D monolayers would be 0.32 and 0.25, respectively. Taken together, these results demonstrate that the overall increase in VinTS and VinTL lifetime (and decrease in FRET efficiency) observed in 3D compared with 2D cultures cannot be accounted for by photobleaching.

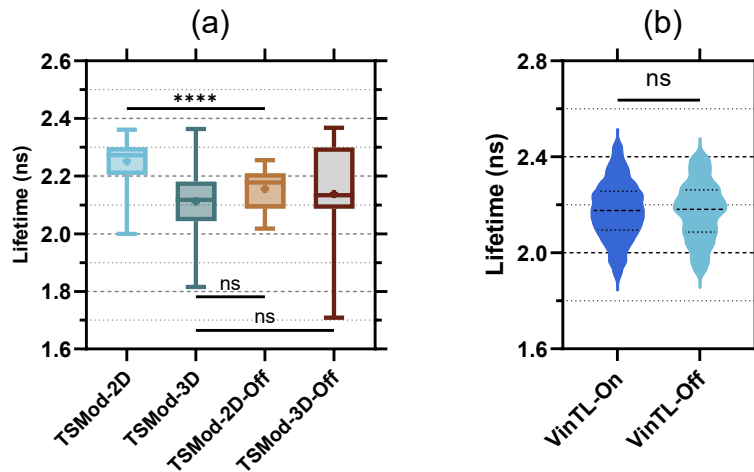


Fig. S4. Photobleaching tests in 2D monolayers and multicellular aggregates (See Supplementary Note 4 above). (a) Photobleaching test of TSMoD in 2D and 3D cultures with the 520nm excitation laser on (TSMoD-2D and TSMoD-3D) or off (TSMoD-2D-Off and TSMoD-3D-Off). \*\*\*\* denotes  $p < 0.0001$  and 'ns' denotes  $p > 0.05$  (Kruskal-Wallis test followed by Dunn's multiple comparisons). Results of multi-comparisons statistics tests may be found in Supplementary Table S5 (Supplementary Note 6 below). The boxes' length is the interquartile range (IQR) extending from the 25<sup>th</sup> to the 75<sup>th</sup> percentile, the line denotes the median, the point the mean, and the whiskers extend to the minimum and maximum value. (b) Photobleaching test of VinTL in 2D monolayers with the 520nm laser turned on (VinTL-On) or off (VinTL-Off). 'ns' denotes  $p > 0.05$  (Mann-Whitney test),  $N = 595$  adhesions in VinTL-on, and  $N = 540$  adhesions in VinTL-Off.

#### 5. Conversion of Apparent FRET to True FRET efficiency:

**Fig. S5** depicts the two-point calibration to convert Apparent FRET efficiency to True FRET Efficiency.

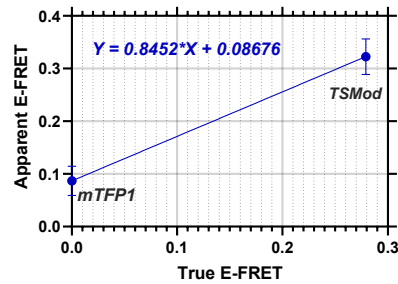


Fig. S5. Two-point calibration using the 3D culture data for mTFP1 and TSMoD.

## 6. Multiple comparisons statistics results

**Table S1: Multiple comparisons, Fig. 4(a), Y-compound treatment in 2D monolayers**  
*Fisher's LSD test*

Test details	P Value
VinTL control vs. VinTL Y treated	0.5000
VinTL control vs. VinTL Y treated	<b>0.0383</b>
VinTL Y treated vs. VinTS Y treated	0.4032

**Table S2: Multiple comparisons, Fig. 4(b), Y-compound treatment in 3D aggregates**  
*Fisher's LSD test*

Test details	P Value
VinTL control vs. VinTL Y treated	0.5799
VinTL control vs. VinTL Y treated	<b>0.0187</b>
VinTL Y treated vs. VinTS Y treated	0.0814

**Table S3: Multiple comparisons, Fig. 5(c), lifetime of mTFP1 and TSMoD**  
*Dunn's test*

Test details	P Value
mTFP1-2D vs. TSMoD-2D	<0.0001
mTFP1-3D vs. TSMoD-3D	<0.0001
TSMoD-2D vs. TSMoD-3D	<0.0001

**Table S4: Multiple comparisons, Fig. 5(d). FRET efficiency in 2D and 3D cultures.**  
*Tukey's test*

Test details	P Value
2D Culture VinTL vs. 2D Culture VinTS	0.0300
2D Culture VinTL vs. 3D Culture VinTL	0.0419
2D Culture VinTS vs. 3D Culture VinTS	0.0053
3D Culture VinTL vs. 3D Culture VinTS	0.0087

**Table S5: Multiple comparisons, Fig. S4 (a), TSMoD photobleaching test**  
*Dunn's test*

Test details	P Value
TSMoD-2D vs. TSMoD-2D-Off	<0.0001
TSMoD-3D vs. TSMoD-3D-Off	0.0926
TSMoD-3D vs. TSMoD-2D-Off	0.2716